PLOS PATHOGENS

REVIEW

Assembly and transport of filovirus nucleocapsids

Olga Dolnik*, Stephan Becker*

Institute of Virology, Philipps-University Marburg, Marburg, Germany

* dolnik@staff.uni-marburg.de (OD); becker@staff.uni-marburg.de (SB)

Abstract

Filovirus-infected cells are characterized by typical cytoplasmic inclusion bodies (IBs) located in the perinuclear region. The formation of these IBs is induced mainly by the accumulation of the filoviral nucleoprotein NP, which recruits the other nucleocapsid proteins, the polymerase co-factor VP35, the polymerase L, the transcription factor VP30 and VP24 via direct or indirect protein–protein interactions. Replication of the negative-strand RNA genomes by the viral polymerase L and VP35 occurs in the IBs, resulting in the synthesis of positive-strand genomes, which are encapsidated by NP, thus forming ribonucleoprotein complexes (antigenomic RNPs). These newly formed antigenomic RNPs in turn serve as templates for the synthesis of negative-strand RNA genomes that are also encapsidated by NP (genomic RNPs). Still in the IBs, genomic RNPs mature into tightly packed transport-competent nucleocapsids (NCs) by the recruitment of the viral protein VP24. NCs are tightly coiled left-handed helices whose structure is mainly determined by the multimerization of NP at its N-terminus, and these helices form the inner layer of the NCs. The RNA genome is fixed by 2 lobes of the NP N-terminus and is thus guided by individual NP molecules along the turns of the helix. Direct interaction of the NP C-terminus with the VP35 and VP24 molecules forms the outer layer of the NCs. Once formed, NCs that are located at the border of the IBs recruit actin polymerization machinery to one of their ends to drive their transport to budding sites for their envelopment and final release. Here, we review the current knowledge on the structure, assembly, and transport of filovirus NCs.

Citation: Dolnik O, Becker S (2022) Assembly and transport of filovirus nucleocapsids. PLoS Pathog 18(7): e1010616. https://doi.org/10.1371/journal.ppat.1010616

Editor: Rachel Fearns, Boston University, UNITED STATES

Published: July 28, 2022

Funding: This study was funded by the Deutsche Forschungsgemeinschaft (DFG) through the Sonderforschungsbereich SFB 1021 project A05 to SB. The funders had no role in study design, data collection and analysis, decision to publish, or preparation of the manuscript.

Competing interests: The authors have declared that no competing interests exist.

1. Introduction

Ebolavirus (EBOV) and *Marburgvirus* (MARV) represent 2 genera of the family *Filoviridae*, which includes important zoonotic pathogens. EBOV and MARV cause fatal outbreaks in humans with case fatality rates of up to 90% [1]. Because of their nonsegmented single-stranded RNA genome that has negative polarity, filoviruses belong to the order *Mononegavirales*. Filovirus particles have a characteristic filamentous shape that is approximately 1 μm in length and a diameter of approximately 90 nm. The viral genome is encapsidated by the nucleoprotein NP and is associated with 4 additional viral proteins (VP): VP35 (the analog of the P protein in other mononegaviruses), the polymerase L, the transcription factor VP30 and VP24, forming the nucleocapsid (NC). The matrix protein VP40 surrounds the NC, forming a

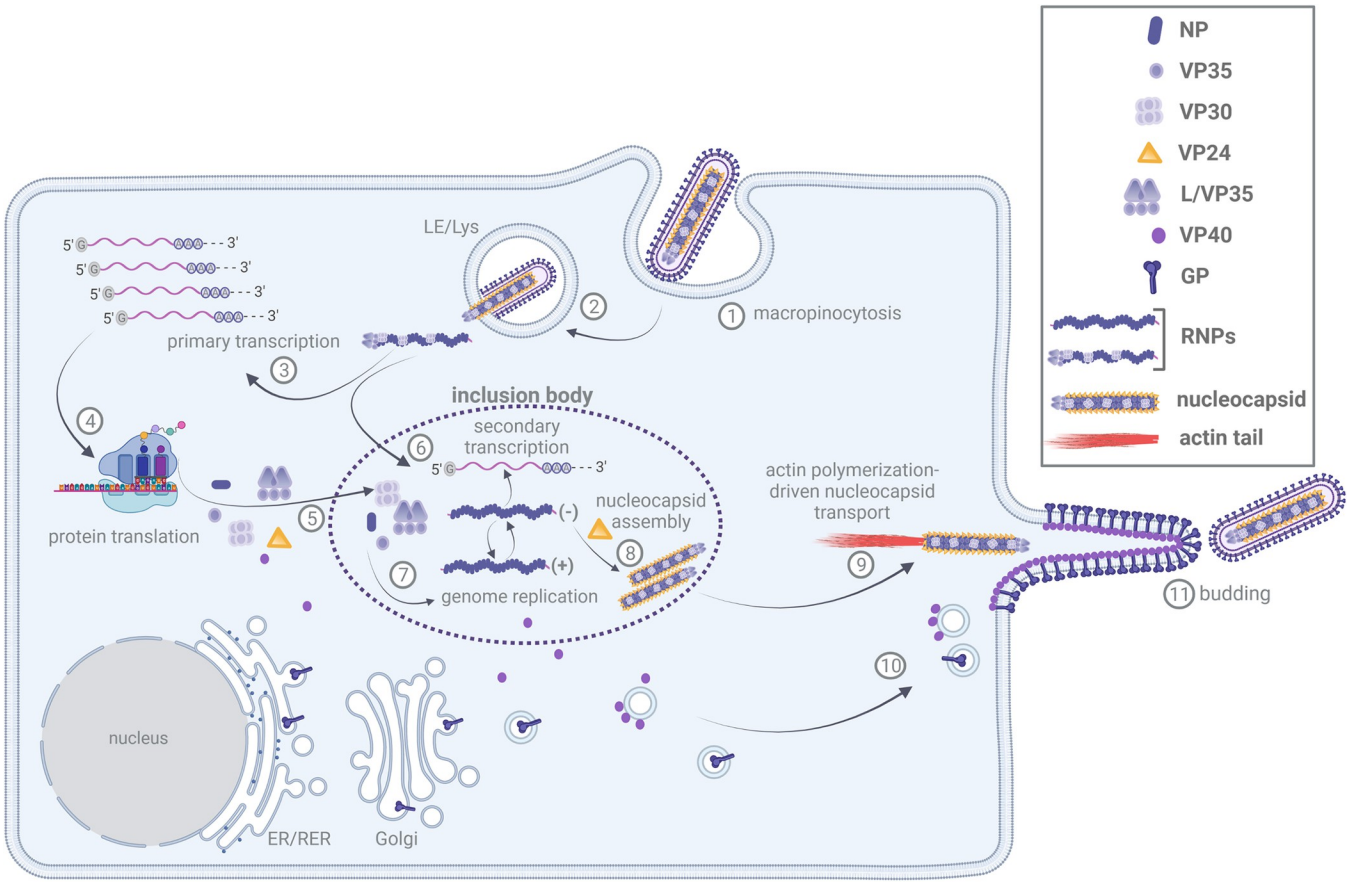

Fig 1. Filovirus replication cycle. Viral entry into target cells is initiated after attachment to the plasma membrane and is accomplished by macropinocytosis (1). During maturation of macropinocytic vesicles into LE/Lys, the viral envelope fuses with the LE/Lys membrane, and the NC is released into the cytosol (2), where it serves as a template for the primary transcription of capped viral mRNAs (3). Translation of viral proteins (4) occurs at free ribosomes, with the exception of GP, which is translated at the rough endoplasmatic reticulum (ER/RER). GP is transported through the classical secretory pathway via the Golgi apparatus to the plasma membrane. The matrix protein VP40 associates with membrane vesicles and is transported to the plasma membrane to form the viral envelope together with GP and cellular lipids (10). Expression of NC proteins (NP, VP35, VP30, VP24, and L) leads to the formation of IBs (5) where secondary transcription (6), genome replication (7), and NC assembly are organized (8). NCs are transported directionally from IBs to budding sites through actin polymerization-driven transport mediated by actin tail formation at one end (9). Envelopment of NCs by membranes containing VP40 and GP occurs at the plasma membrane where budding of filoviruses take place (11). Figure was created with BioRender.com. IB, inclusion body; LE/Lys, late endosomes/lysosomes; RER, rough endoplasmatic reticulum; RNP, ribonucleoprotein complex.

https://doi.org/10.1371/journal.ppat.1010616.g001

regular layer beneath the viral envelope. The glycoprotein GP is incorporated into the viral envelope [2]. The entry of viral particles into cells is initiated by the recognition of target cells by GP, and entry is mediated by macropinocytosis (Fig 1) [3,4]. During endocytosis, macropinocytic vesicles mature into late endosomes/lysosomes, where GP is cleaved by cellular proteases. This process exposes the receptor-binding domain of GP to the endosomal receptor NPC1, and receptor binding initiates fusion of the viral and lysosomal membranes, which results in the release of NCs into the cytosol [5]. Here, the NC-associated polymerase complex, which consists of L, the polymerase cofactor VP35, and the transcription initiation factor VP30, initiates the primary transcription of viral mRNAs. Except for GP, which is translated at ER-bound ribosomes and transported through the classical secretory pathway to the plasma membrane, all the other viral proteins are translated at free ribosomes in the cytosol. Increasing amounts of viral proteins in the cytosol lead to the formation of inclusion bodies (IBs), which are a hallmark of filovirus infection [6,7]. IBs represent sites of secondary transcription,

genome replication, and de novo NC formation of transport-competent NCs that are transported to budding sites at the plasma membrane for envelopment (Fig 1) [8–12]. In the literature, the term NC is often used equivalently to the term ribonucleoprotein complex (RNP). In this review, we consider RNPs as functional complexes composed of viral RNA, NP, VP35, L, and VP30 that are active in transcription or replication [13]. Therefore, RNPs can have different protein compositions consisting of the viral RNA, NP, VP35, and L with or without the transcription initiation factor VP30. In comparison, NCs are defined as discrete condensed structures that are also detected inside the viral particles composed of the genomic RNA, NP, VP35, L, VP30, and VP24 (Fig 1). The complete replication cycle of filoviruses was reviewed by Kolesnikova and colleagues [14]. Here, we review the current knowledge on the structure, assembly, and transport of filovirus NCs from their assembly site in IBs to the budding sites at the plasma membrane, where they are packaged into filamentous infectious virions.

2. Structural components of filovirus nucleocapsids

The current structural model of the filoviral NC is based on data obtained by transmission electron microscopy (EM), cryo-electron microscopy (Cryo-EM), cryo-electron tomography (Cryo-ET), and 3D reconstruction methods, such as subtomogram averaging and mapping of available crystal structures onto obtained electron densities (Fig 2) [15].

The main determinant of the structure of filovirus NCs is the nucleoprotein NP, whose homo-oligomerization results in the formation of helical structures [6,16,17]. Transmission electron microscopy analyses of ectopically expressed NP showed that the hydrophobic N-terminal domain of NP (for EBOV amino acids 1–450 and for MARV amino acids 1–394, NP_{NTD}) represents the minimal structural component responsible for NP oligomerization. NP_{NTD} oligomerization results in the formation of helices with a diameter of 28 nm corresponding to the inner ring of cross-sectioned NCs [18–21]. Cryo-ET of NP_{NTD} helices and averaging techniques revealed that the first 450 N-terminal amino acids of NP are divided into an N-terminal and a C-terminal lobe connected by a flexible hinge region (Fig 2A). A positively charged binding cleft in NP_{NTD} mediates the binding of the negatively charged RNA by electrostatic interactions [15,22–26]. Each NP monomer in the left-handed NP helix covers 6 nucleotides of the genome. The length of MARV virions is 876 nm, and that of EBOV virions is 1,028 nm; however, the sizes of their genomes are similar, namely 19,111 and 18,961 bases, respectively [25,27,28]. The different lengths of the MARV and EBOV virions are the result of the different amounts of NP molecules per rung of the NC helix leading to the differences in the diameters. The inner diameter of the MARV NC is 32 nm, which corresponds to 29.6 NP molecules. In the case of EBOV, the inner diameter of the NC helix is smaller than that of MARV, namely, 28 nm, and corresponds to an average of 24.6 NP molecules per rung. Thus, EBOV NCs have to be longer to package the whole genome. Therefore, the different diameters and corresponding lengths of the NCs determine the lengths of the viral particles [25,27,28].

The NP helix is stabilized by bound RNA as well as by interactions between the N-terminal arm-region of one NP molecule (amino acids 1–24 for EBOV and 1–19 for MARV) and the C-terminal lobe of the adjacent NP molecule within one rung of the helix (Fig 2A). Inter-rung contacts between NP molecules are formed between the C- and N-terminal regions of NP_{NTD} (Fig 2B) [15,24–26].

The hydrophilic C-terminal domain of NP (NP_{CTD}) consists of an intrinsically disordered linker region and a structured tail region (NP_{Ct}) that extends from the inner helix formed by NP_{NTD} [27–32]. It has been shown that NP_{CTD} disrupts the tight condensation of the NP_{NTD} helix leading to formation of loosely coiled helices [27]. Recent analysis using molecular dynamics simulation revealed different stabilities of NP-NP interactions throughout the helix,

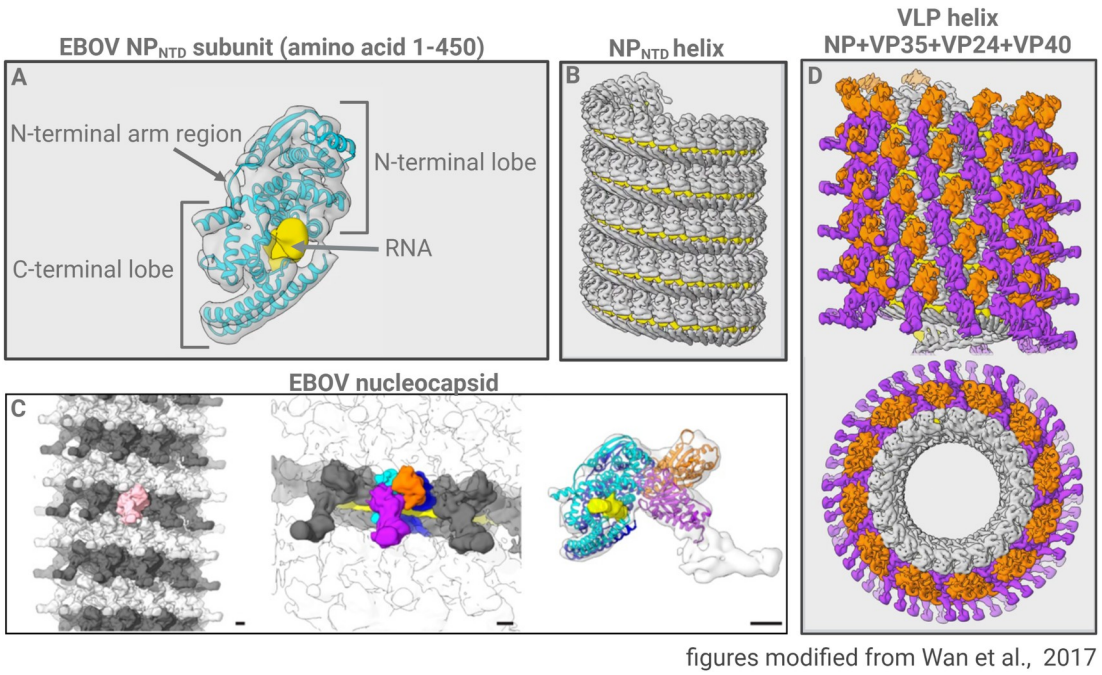

Fig 2. Structure of Ebola virus nucleocapsids [15]. (**A**) NP$_{NTD}$ monomer (amino acid 1–450) derived from subtomogram averaging of NP$_{NTD}$ helices (see B) with the aligned crystal structure in cyan and the putative RNA binding site in yellow. An arrow indicates the N-terminal arm region with the N-terminal helix. (**B**) The left-handed NP$_{NTD}$ helix bound to an RNA chain (yellow). (**C**) Model of the EBOV NC derived from Cryo-ET and subtomogram averaging. Left: NC structure of EBOV. Subunits of 1 rung are shown in dark or light gray. One subunit is highlighted in pink. Middle: The NP$_{NTD}$ subunits are highlighted in cyan and blue, the structures highlighted in orange, and purple are NP$_{CTD}$ protrusions, 2 VP24 molecules and VP35. The bound RNA is highlighted in yellow. Right: side view of the asymmetric protomer showing 2 molecules of NP$_{NTD}$ (cyan and blue), 2 molecules of VP24 (orange and purple), and unassigned densities most likely corresponding to NP$_{CTD}$ and VP35 (light gray). (**D**) Structure of recombinant EBOV NC obtained from virus-like particles composed of NP, VP35, VP24, and VP40. Top: longitudinal presentation of the helix; bottom: cross-section of the helix. The boomerang-shaped protrusions are highlighted in purple, and small protrusions are highlighted in orange. The inner layer composed of NP$_{NTD}$ is shown in gray. Figures are modified from Wan and colleagues [15]. Figure was created with BioRender.com. Cryo-ET, cryo-electron tomography; NC, nucleocapsid.

https://doi.org/10.1371/journal.ppat.1010616.g002

suggesting high flexibility, especially at the ends of the helix [33]. While NP$_{NTD}$ is relatively conserved among the family *Filoviridae*, NP$_{CTD}$ is more divergent, especially in the tail region. NP$_{CTD}$ has been shown to mediate important interactions with other viral and cellular proteins [34–39].

In the presence of VP35 and VP24, the loosely coiled NP-helices change to condensed and rigid helical structures (Fig 3B) [18,20,27]. Immunocryo-EM analyses of the helical NC within filoviral particles revealed the positions of the NC-associated proteins NP, VP35, and VP24 on vertical slices of NCs, showing that in EBOV, NP forms an inner layer with a diameter of approximately 28 nm that resembles the helix formed by NP$_{NTD}$. VP35 and VP24 were observed outside the inner NP layer [27,28,31]. Recent detailed Cryo-ET analyses combined with subtomogram averaging revealed that the overall structure of the NC inside the viral particles is a tube-like cylinder composed of aligned NP$_{NTDs}$ with boomerang-shaped protrusions consisting of NP$_{CTD}$, VP35, and VP24 (Fig 2C) [15,27,31]. Consistent with these observations, the ectopic coexpression of NP, VP35, and VP24 resulted in the formation of NC-like structures (NCLS) with the same symmetry and structure as the NCs in virions but with more variable lengths (Fig 2D) [15,27,31]. The localization of the functional polymerase complex consisting of VP35 and L and that of the transcription factor VP30 in the viral NC are thus far unresolved, possibly because these proteins are scattered over the NC. Interestingly, Cryo-ET

revealed that the NCs possess a pointed and a barbed end, which complemented the observation that NC budding is always directional with the pointed end in front [27,28,40].

3. Inclusion bodies as de novo nucleocapsid assembly sites

3.1. IBs formation

A hallmark of filovirus-infected cells is the formation of IBs, which, in EM analyses, appear as the accumulation of thin-walled, apparently flexible helices and more rigid thick-walled, electron-dense helices embedded in a matrix of viral and cellular proteins (Fig 3C) [6,7,20,41,42]. For many years, whether IBs performed a function in the viral replication cycle or whether IBs

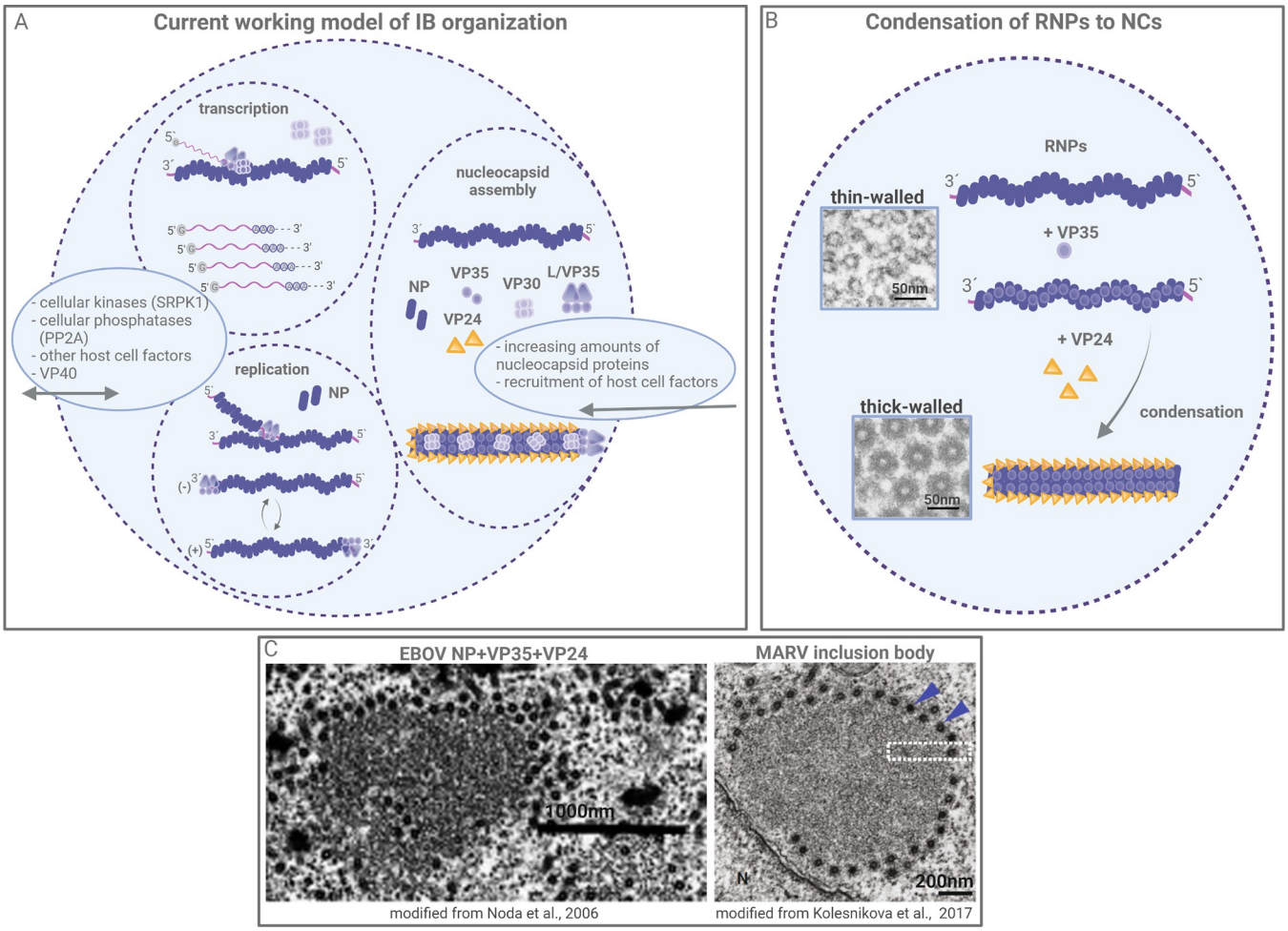

Fig 3. Filovirus inclusion bodies. (**A**) Current working model of IB organization. Transcription and genome replication occur inside IBs. It is possible that the 2 activities are separated in different subcompartments which, however, remains to be investigated. Possible subcompartmentalization of IBs might result from liquid–liquid phase separation based on RNA and protein concentrations. Regulation of viral transcription is partially based on the phosphorylation status of VP30, which modulates interactions with the polymerase cofactor VP35 and the polymerase L. VP30 phosphorylation is regulated by host cell kinases and phosphatases whose localization and availability might be interdependent. Increasing levels of NC proteins and possibly the recruitment of VP40 and/or host cell factors into IBs is thought to trigger the assembly of NCs. (**B**) Model of RNPs condensation to NCs in IBs. Electron micrographs from Noda and colleagues [20] show thin-walled helices upon NP expression and thick-walled helices upon coexpression of NP+VP35+VP24. The thin-walled helices detected inside IBs may represent RNPs that are active in transcription or replication or may represent intermediates of assembly. (**C**) Left picture: Electron micrograph from Noda and colleagues [20] of an IB (left) upon coexpression of EBOV NP, VP35, and VP24 showing cross-sectioned NCLS. Right picture: Electron micrograph from Kolesnikova and colleagues [14] of an IB from a MARV-infected cell with cross-sectioned NCs. Blue arrowheads indicate condensed thick-walled NCs at the periphery of the IB. Figure was created with BioRender.com. IB, inclusion body; NC, nucleocapsid; NCLS, NC-like structure; RNP, ribonucleoprotein complex.

https://doi.org/10.1371/journal.ppat.1010616.g003

represented dead-end accumulations of viral material remained under debate. Investigations in the last decade, however, revealed that viral IBs represent membrane-less virus-induced compartments with high structural and functional dynamics that are similar to cellular membrane-less compartments called liquid organelles [43–45]. Although not systematically proven, it is very likely that filovirus IBs also represent liquid or liquid-like organelles formed by liquid–liquid phase separation, similar to IBs of other mononegaviruses as reviewed in [46]. For example, disassembly and reassembly of IBs in EBOV-infected cells during cell division is a typical feature of liquid organelles and has been shown in live-cell imaging experiments [11,46]. Further live-cell imaging experiments revealed the shape of IBs to be highly dynamic and their size is also determined by fusion and fission events [9,10]. It was previously shown that transient expression of filovirus NP on its own could induce the formation of IBs [6,47,48]. Truncation of NP at the N-terminus or the C-terminus resulted in inhibition of IBs formation [35,36]. Interestingly, coexpression of VP35 with NP constructs that were unable to form IBs ($NP_{\Delta Ct}$) can rescue IBs formation, suggesting that the interaction of NP and VP35 can control the early steps of this process [35]. Both NP and VP35 share characteristic properties of proteins that form liquid organelles, such as intrinsically disordered domains, multivalency, phosphorylation, and RNA-binding ability [43]. Liquid–liquid phase separation might be necessary to create a protected environment inside the infected cell to enable replication and transcription as well as NC assembly [49].

3.2. NC-assembly steps in the IBs

Currently, the precise order of the processes leading to the formation of NCs inside of IBs is still unknown. Similarly, while transcription and replication of filovirus RNA take place inside IBs, it is not clear how these 2 processes are separated in time and space from NC assembly (Fig 3A) [11,12]. Based on the available data, we suggest the following model of RNP formation and NC assembly (Fig 3A and 3B).

It has been shown that an N-terminal peptide of VP35 functions as a chaperone that maintains NP in a monomeric state before the oligomerization of NP and encapsidation of the viral RNA occurs concomitantly to replication [50–52]. The interaction of the 2 proteins is complex and involves several interaction domains on NP and VP35 [13,42,47,50,51,53,54]. Although it is currently unknown when during the viral RNA synthesis VP35 is recruited to the NP-RNA complex, a stoichiometric ratio of the 2 proteins has been shown to be crucial for the formation of thin-walled helices that are detected in the filoviral IBs [20,42]. Electron microscopy so far was not able to distinguish thin-walled helices composed of NP-VP35-RNA or NP-RNA. It is also not known which of the 2 complexes serves as template for RNA synthesis by the viral polymerase (Fig 3B and 3C). Similar to other mononegaviruses, the functional polymerase composed of VP35 and L is recruited to IBs via the interaction between NP and VP35 to enable RNA synthesis [8,11,12,53,55–57]. The positions of the polymerase complex inside NCs in not known so far. It has been shown that VP30 is recruited into IBs by direct interactions with NP; however, its position in the NC is also unresolved [50,58–61].

3.3. Separation of transcription and replication in IBs

While replication of filoviral genomes requires the presence of NP, VP35, and L, transcription is dependent on the transcriptional initiation factor VP30 [62]. The transcriptional support activity of VP30 is switched off upon phosphorylation. Thus, phosphorylation of VP30 regulates the balance between transcription and replication [63–65]. Phosphorylation of VP30 also regulates its interaction with NP and is mediated by the cellular kinase SRPK1, and dephosphorylation is catalyzed by PP2A. Both the phosphorylation and dephosphorylation of VP30

occur in IBs, demonstrating the importance of host cell factors for the regulation of viral mRNA transcription and replication in IBs [39,59,65]. Additionally, it was shown that the interaction of VP30 with the polymerase cofactor VP35 modulates transcription and that VP30 can interact directly with L [48,64]. Although it is not known exactly how the switch from transcription to replication is mediated, the current data suggest that posttranslational protein modifications, such as phosphorylation, influence protein–protein, and/or protein–RNA interactions and thus regulate this process (Fig 3A) [63,64]. Increasing levels of NP and VP35 and possibly increasing levels of phosphorylated VP30 in IBs may also activate replication of the viral genome. Further in vitro transcription/replication studies are needed to answer these remaining questions.

It is currently unknown how the transcription and replication of viral RNA are temporally and spatially organized inside filoviral IBs. An interesting observation made by Nelson and colleagues in EBOV-infected cells already indicated potential IBs subcompartments when distinct granules were detected within IBs containing EBOV NP mRNA together with eIF3 and other stress granule-associated (SG) proteins [66]. Sequestration of SG-associated proteins into IBs has been suggested to interfere with the activation of the innate immune system [67–69]. Interestingly, for respiratory syncytial virus (RSV), transient formation of granules inside IBs was observed that contained viral mRNA and the viral transcription anti-terminator protein M2-1 but not the other viral proteins involved in RNA synthesis, the nucleoprotein N, phosphoprotein P or L [70]. It remains to be investigated if filovirus IBs possess an internal organization that leads to transient sequestration of viral mRNA as well. Likewise, the details of spatiotemporal organization of filovirus transcription and replication and NC maturation has yet to be resolved (Fig 3A).

3.4. RNP condensation to NCs

The maturation of thin-walled helices (RNPs) into thick-walled helices (corresponding to NCs) can only be observed in the presence of VP35 and VP24, and thick-walled helices are detected mainly in the periphery of IBs (Fig 3B and 3C) [16,18–20,36]. High levels of VP24 inhibit transcription and replication, suggesting that increasing levels of VP24 in IBs block viral RNA synthesis in favor of NC maturation [71–76]. VP24 is recruited into IBs by interaction with NP [16,19,20,71,72,74,75]. Recently, it was demonstrated that EBOV VP24 can be SUMOylated and ubiquitinated and undergoes nucleocytoplasmic shuttling [77,78]. Whether posttranslational modification regulates the recruitment of VP24 into IBs and/or its functions in NC condensation and transport remains to be determined.

4. Transport of nucleocapsids from inclusion bodies to budding sites

The ectopic expression of fluorescently labeled VP30 (VP30-GFP) in EBOV- or MARV-infected cells results in fluorescently labeled NCs, whose movement can be monitored by live-cell imaging. Using this approach, the ejection of single NCs from IBs could be observed, and their intracellular transport to the plasma membrane could be tracked and characterized in living cells [9,10].

Since the long filovirus NC cannot reach the budding site by diffusion alone, interactions with host cell factors are required to mediate its transport. The application of cytoskeleton-depolymerizing drugs revealed that the transport of filovirus NCs is driven by an actin-dependent mechanism [9,10,79,80]. Other intracellular pathogens, such as *Listeria monocytogenes* or baculovirus, express proteins that directly interact with actin and the actin polymerization complex Arp2/3 to promote the polymerization of branched actin filaments [81]. Such

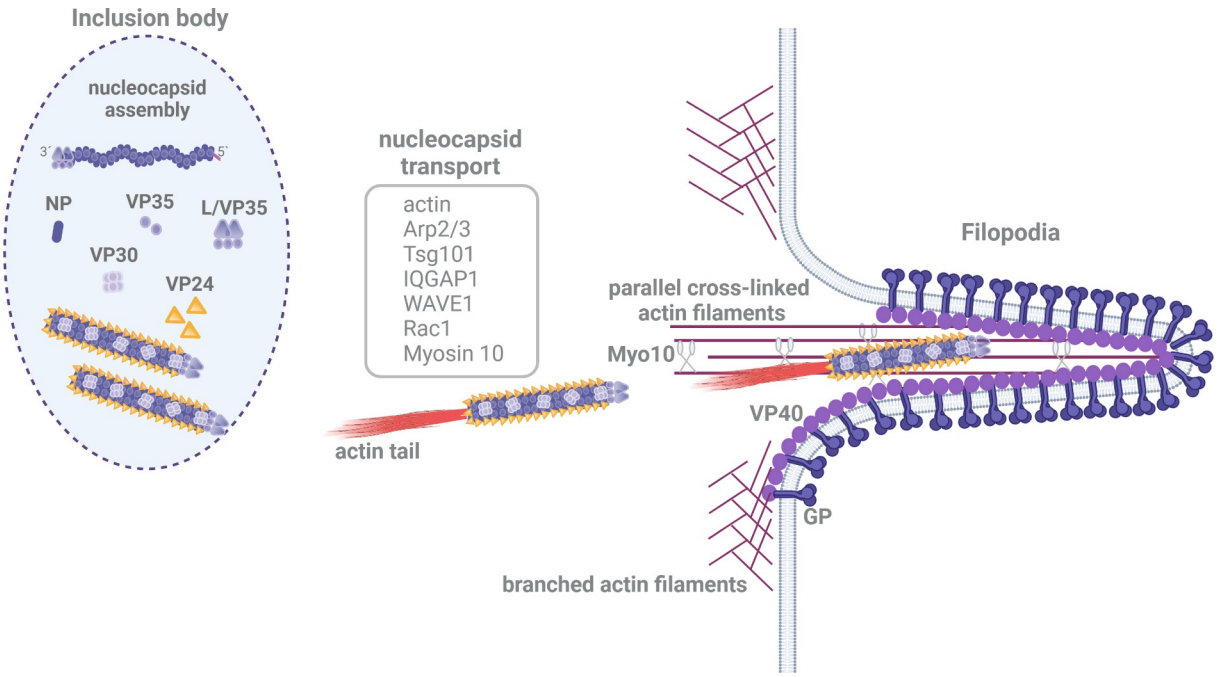

Fig 4. Transport of nucleocapsids from inclusion bodies to budding sites. Transport-competent NCs composed of all the NC proteins are formed inside IBs. The involvement of different host cell factors is required for the actin-dependent transport of NCs (gray box). Outside the IBs, actin tails are formed at one end of the NC in the cytosol, which drive their transport. After reaching the plasma membrane, budding of filoviruses occurs mainly at filopodia, in which myosin 10 may support the transport of NCs along parallel actin filaments. Figure was created with BioRender.com. IB, inclusion body; NC, nucleocapsid.

https://doi.org/10.1371/journal.ppat.1010616.g004

nucleation-promoting factors are required for the activation of the Arp2/3 complex to mediate actin polymerization [81,82]. Direct interactions between filovirus NC proteins and actin or the Arp2/3 complex have not yet been described. To promote actin polymerization for their transport, filovirus NCs may therefore recruit cellular nucleation-promoting factors, which provide a link to actin and the Arp2/3 complex (Fig 4).

Using specific inhibitors and silencing host cell factor expression by siRNA, it was demonstrated that the Arp2/3 complex, WAVE1 and Rac1 play important roles in the actin-dependent transport of NCLS and authentic viral NCs [9,10,83]. Moving filoviral NCLS and NCs display actin comet tails at one end, suggesting a transport mechanism previously described for the intracellular transport of vaccinia virus and baculovirus capsids that is based on the polymerization of branched actin filaments [81,84]. The NP of MARV was shown to recruit cellular factors into the IBs, such as Tsg101 and IQGAP1, a regulator of actin dynamics and filopodia formation, which is also involved in regulating the transport of NCs. Down-regulation of Tsg101 or IQGAP1 expression affected the transport of NCs, resulting in their accumulation close to the plasma membrane and reduced budding at filopodia suggesting different transport steps of NCs from the IBs at first to the planar plasma membrane and then further into filopodia [85]. Filopodia that are enriched with VP40 are the preferred budding sites of filoviruses [9,10,85,86]. This is consistent with data showing that EBOV VP40 strongly enhances the recruitment of NCLS into filopodia [79]. Filopodia are long, thin cellular protrusions containing characteristic parallel actin filaments that are cross-linked by fascin [87]. Unconventional myosin 10 mediates the transport of cargo along actin filaments within filopodia. Myosin 10 was shown to transport VP40, and it is hypothesized that NCs make use of this mechanism for transport inside filopodia (Fig 4) [9,10,86,88]. The exact molecular interactions

between actin polymerization complexes that drive the actin-dependent transport of the NC and the viral NC proteins remain to be determined. Using a minimalistic live-cell imaging system based on fluorophore-tagged NC proteins, it was shown that NP, VP35, and VP24 are essential and sufficient for forming electron-dense and transport-competent helical NCLS [16,18–20,36,71,79,80]. Mutation of the YxxL motif of VP24 in EBOV resulted in NCLS that exhibited significantly impaired transport by an unknown mechanism [89]. Taken together, the current literature demonstrates that both NP and VP24 seem to regulate the actin-dependent transport of NCLS via different mechanisms. Further experiments with the minimalistic live-cell imaging system and application of advanced NC-tracking software are needed to define the molecular mechanism underlying the formation of the actin tail at one end of NCLS that drives their transport.

Different transport kinetics were described for filovirus NCs depending on their intracellular location. The velocities range from 100 nm/s in the filopodia to 400 nm/s in the cytosol, and these differences suggest the involvement of different actin-based transport machineries during transport from IBs to budding sites [9,10,79,80]. The molecular details of the observed differences in the transport velocities of NCs are still unclear. In addition to actin tail-driven transport, NCs were observed to move along actin filaments, suggesting motor protein-dependent and motor protein-independent transport mechanisms [10]. For measles virus, the transport of RNPs from IBs to the plasma membrane is dependent on actin filaments, whereas their incorporation into new virions requires actin dynamics at the cell periphery [90]. Transport kinetics and cytoskeleton inhibitor studies of NCs of other mononegaviruses, such as vesicular stomatitis virus, revealed the involvement of microtubule- and actin-dependent transport mechanisms [91]. Most likely, microtubule-dependent transport does not play a major role in the transport of filovirus NC [9,10,79,80].

The formation of an actin tail at one end of the filovirus NC resulted in directional transport and budding of the particles with the pointed end of the NC in front. It is unknown how the binding of the actin polymerization machinery to one end of the NC is regulated. For example, it was shown that positioning the baculoviral proteins p78/83 or VP80 at one end of the NC influenced the directionality of transport [92–94]. Thus, the structural polarity of the filovirus NC may be the result of the recruitment of the cellular actin polymerization machinery to the barbed end, since budding was shown to occur with the pointed end first (Fig 4) [28,40]. It is tempting to hypothesize that the position of the viral polymerase complex in the NC at the 3′ end of the genome, where it can initiate primary transcription as shown for other mononegaviruses, may influence the recruitment of transport machinery [95,96]. For vesicular stomatitis virus, however, super-resolution imaging revealed that the viral polymerase is located at the blunt end of the bullet-shaped particles where the 5′ end of the genome is located [97]. The viral determinants responsible for recruitment of the actin polymerization machinery at one end of the NC remain to be identified using super-resolution techniques and live-cell imaging.

Interactions of the matrix protein VP40 with NP in the IBs inhibit viral transcription and replication possibly by partial NC condensation and on the other hand enable NC envelopment at the plasma membrane and budding [27,38,73,98,99]. Live-cell imaging studies of MARV-infected cells revealed that outside of IBs association of VP40 with NCs was detected only at the plasma membrane, arguing against a contribution of VP40 to the transport of NCs from IBs to the plasma membrane [10]. The incorporation of NCLSs into infectious virus-like particles (also referred to as transcription and replication competent virus-like particles, trVLPs) at the plasma membrane was dependent on tyrosine phosphorylation of VP40, which occurs at cellular membranes, indicating that docking of NCLS to the plasma membrane and envelopment are regulated by the posttranslational modification of VP40 [98].

5. Conclusions and perspectives

Current data suggest that NP is a highly dynamic protein that organizes protein–protein and protein–RNA interactions to promote RNP and NC formation. The resulting helical structure with boomerang-shaped protrusions has a pointed and a barbed end, generating structural asymmetry. The complete 3D structure showing the location of all NC proteins remains to be solved, which will require high-resolution Cryo-EM and Cryo-ET studies and structure reconstruction methods based on authentic viruses and trVLPs.

The assembly of NCs occurs in NP-induced IBs, which are likely liquid-like organelles. Posttranslational modifications of viral NC proteins, such as phosphorylation and interactions with host cell factors, seem to regulate their formation. Techniques used in liquid organelle biology have to be applied to investigate the liquid–liquid and liquid–solid phase transitions in IBs formation and to further dissect the role of the different viral and cellular factors involved.

NP, VP35, and VP24 are sufficient and essential for forming mature and transport-competent NCs, which require the recruitment of actin polymerization factors for transport from the IBs to budding sites. RNA labeling techniques, multicolor live-cell imaging, and super-resolution imaging and techniques such as correlative light electron microscopy can help to identify the molecular determinants of the viral and host factors that are involved in the formation and transport of NCs.

References

1. Kuhn JH, Adachi T, Adhikari NKJ, Arribas JR, Bah IE, Bausch DG, et al. New filovirus disease classification and nomenclature. Nat Rev Microbiol. 2019; 17(5):261–263. https://doi.org/10.1038/s41579-019-0187-4 PMID: 30926957
2. Mittler E, Kolesnikova L, Herwig A, Dolnik O, Becker S. Assembly of the Marburg virus envelope. Cell Microbiol. 2013; 15(2):270–284. https://doi.org/10.1111/cmi.12076 PMID: 23186212
3. Nanbo A, Imai M, Watanabe S, Noda T, Takahashi K, Neumann G, et al. Ebolavirus is internalized into host cells via macropinocytosis in a viral glycoprotein-dependent manner. PLoS Pathog. 2010; 6(9): e1001121. https://doi.org/10.1371/journal.ppat.1001121 PMID: 20886108
4. Saeed MF, Kolokoltsov AA, Albrecht T, Davey RA. Cellular entry of ebola virus involves uptake by a macropinocytosis-like mechanism and subsequent trafficking through early and late endosomes. PLoS Pathog. 2010; 6(9):e1001110. https://doi.org/10.1371/journal.ppat.1001110 PMID: 20862315
5. Carette JE, Raaben M, Wong AC, Herbert AS, Obernosterer G, Mulherkar N, et al. Ebola virus entry requires the cholesterol transporter Niemann-Pick C1. Nature. 2011; 477(7364):340–343. https://doi.org/10.1038/nature10348 PMID: 21866103
6. Kolesnikova L, Muhlberger E, Ryabchikova E, Becker S. Ultrastructural organization of recombinant Marburg virus nucleoprotein: comparison with Marburg virus inclusions. J Virol. 2000; 74(8):3899–3904. https://doi.org/10.1128/jvi.74.8.3899-3904.2000 PMID: 10729166
7. Geisbert TW, Jahrling PB. Differentiation of filoviruses by electron microscopy. Virus Res. 1995; 39(2–3):129–150. https://doi.org/10.1016/0168-1702(95)00080-1 PMID: 8837880
8. Nanbo A, Watanabe S, Halfmann P, Kawaoka Y. The spatio-temporal distribution dynamics of Ebola virus proteins and RNA in infected cells. Sci Rep. 2013; 3:1206. https://doi.org/10.1038/srep01206 PMID: 23383374
9. Schudt G, Dolnik O, Kolesnikova L, Biedenkopf N, Herwig A, Becker S, et al. Transport of Ebolavirus Nucleocapsids Is Dependent on Actin Polymerization: Live-Cell Imaging Analysis of Ebolavirus-Infected Cells. J Infect Dis. 2015; 212(Suppl 2):S160–S166. https://doi.org/10.1093/infdis/jiv083 PMID: 26038396
10. Schudt G, Kolesnikova L, Dolnik O, Sodeik B, Becker S. Live-cell imaging of Marburg virus-infected cells uncovers actin-dependent transport of nucleocapsids over long distances. Proc Natl Acad Sci U S A. 2013; 110(35):14402–14407. https://doi.org/10.1073/pnas.1307681110 PMID: 23940347
11. Hoenen T, Shabman RS, Groseth A, Herwig A, Weber M, Schudt G, et al. Inclusion bodies are a site of ebolavirus replication. J Virol. 2012; 86(21):11779–11788. https://doi.org/10.1128/JVI.01525-12 PMID: 22915810

12. Dolnik O, Stevermann L, Kolesnikova L, Becker S. Marburg virus inclusions: A virus-induced microcompartment and interface to multivesicular bodies and the late endosomal compartment. Eur J Cell Biol. 2015; 94(7–9):323–331. https://doi.org/10.1016/j.ejcb.2015.05.006 PMID: 26070789

13. Muhlberger E, Weik M, Volchkov VE, Klenk HD, Becker S. Comparison of the transcription and replication strategies of marburg virus and Ebola virus by using artificial replication systems. J Virol. 1999; 73 (3):2333–2342. https://doi.org/10.1128/JVI.73.3.2333-2342.1999 PMID: 9971816

14. Kolesnikova L, Nanbo A, Becker S, Kawaoka Y. Inside the Cell: Assembly of Filoviruses. Curr Top Microbiol Immunol. 2017; 411:353–380. https://doi.org/10.1007/82_2017_15 PMID: 28601948

15. Wan W, Kolesnikova L, Clarke M, Koehler A, Noda T, Becker S, et al. Structure and assembly of the Ebola virus nucleocapsid. Nature. 2017; 551(7680):394–397. https://doi.org/10.1038/nature24490 PMID: 29144446

16. Huang Y, Xu L, Sun Y, Nabel GJ. The assembly of Ebola virus nucleocapsid requires virion-associated proteins 35 and 24 and posttranslational modification of nucleoprotein. Mol Ther. 2002; 10(2):307–316. https://doi.org/10.1016/s1097-2765(02)00588-9 PMID: 12191476

17. Mavrakis M, Kolesnikova L, Schoehn G, Becker S, Ruigrok RW. Morphology of Marburg virus NP-RNA. Virology. 2002; 296(2):300–307. https://doi.org/10.1006/viro.2002.1433 PMID: 12069528

18. Watanabe S, Noda T, Kawaoka Y. Functional mapping of the nucleoprotein of Ebola virus. J Virol. 2006; 80(8):3743–3751. https://doi.org/10.1128/JVI.80.8.3743-3751.2006 PMID: 16571791

19. Noda T, Halfmann P, Sagara H, Kawaoka Y. Regions in Ebola virus VP24 that are important for nucleocapsid formation. J Infect Dis. 2007; 196(Suppl 2):S247–S250. https://doi.org/10.1086/520596 PMID: 17940956

20. Noda T, Ebihara H, Muramoto Y, Fujii K, Takada A, Sagara H, et al. Assembly and budding of Ebolavirus. PLoS Pathog. 2006; 2(9):e99. https://doi.org/10.1371/journal.ppat.0020099 PMID: 17009868

21. Fujita-Fujiharu Y, Sugita Y, Takamatsu Y, Houri K, Igarashi M, Muramoto Y, et al. Structural insight into Marburg virus nucleoprotein-RNA complex formation. Nat Commun. 2022; 13(1):1191. https://doi.org/10.1038/s41467-022-28802-x PMID: 35246537

22. Dong S, Yang P, Li G, Liu B, Wang W, Liu X, et al. Insight into the Ebola virus nucleocapsid assembly mechanism: crystal structure of Ebola virus nucleoprotein core domain at 1.8 Å resolution. Protein Cell. 2015; 6(5):351–362. https://doi.org/10.1007/s13238-015-0163-3 PMID: 25910597

23. Zhu T, Song H, Peng R, Shi Y, Qi J, Gao GF, et al. Crystal Structure of the Marburg Virus Nucleoprotein Core Domain Chaperoned by a VP35 Peptide Reveals a Conserved Drug Target for Filovirus. J Virol. 2017; 91(18). https://doi.org/10.1128/JVI.00996-17 PMID: 28659479

24. Su Z, Wu C, Shi L, Luthra P, Pintilie GD, Johnson B, et al. Electron Cryo-microscopy Structure of Ebola Virus Nucleoprotein Reveals a Mechanism for Nucleocapsid-like Assembly. Cell. 2018; 172(5):966–978.e12. https://doi.org/10.1016/j.cell.2018.02.009 PMID: 29474922

25. Sugita Y, Matsunami H, Kawaoka Y, Noda T, Wolf M. Cryo-EM structure of the Ebola virus nucleoprotein-RNA complex at 3.6 A resolution. Nature. 2018; 563(7729):137–140. https://doi.org/10.1038/s41586-018-0630-0 PMID: 30333622

26. Kirchdoerfer RN, Saphire EO, Ward AB. Cryo-EM structure of the Ebola virus nucleoprotein-RNA complex. Acta Crystallogr F Struct Biol Commun. 2019; 75(Pt 5):340–347. https://doi.org/10.1107/S2053230X19004424 PMID: 31045563

27. Bharat TA, Noda T, Riches JD, Kraehling V, Kolesnikova L, Becker S, et al. Structural dissection of Ebola virus and its assembly determinants using cryo-electron tomography. Proc Natl Acad Sci U S A. 2012; 109(11):4275–4280. https://doi.org/10.1073/pnas.1120453109 PMID: 22371572

28. Bharat TA, Riches JD, Kolesnikova L, Welsch S, Krahling V, Davey N, et al. Cryo-electron tomography of Marburg virus particles and their morphogenesis within infected cells. PLoS Biol. 2011; 9(11): e1001196. https://doi.org/10.1371/journal.pbio.1001196 PMID: 22110401

29. Baker LE, Ellena JF, Handing KB, Derewenda U, Utepbergenov D, Engel DA, et al. Molecular architecture of the nucleoprotein C-terminal domain from the Ebola and Marburg viruses. Acta Crystallogr D Struct Biol. 2016; 72(Pt 1):49–58. https://doi.org/10.1107/S2059798315021439 PMID: 26894534

30. Dziubanska PJ, Derewenda U, Ellena JF, Engel DA, Derewenda ZS. The structure of the C-terminal domain of the Zaire ebolavirus nucleoprotein. Acta Crystallogr D Biol Crystallogr. 2014; 70(Pt 9):2420–2429. https://doi.org/10.1107/S1399004714014710 PMID: 25195755

31. Beniac DR, Melito PL, Devarennes SL, Hiebert SL, Rabb MJ, Lamboo LL, et al. The organisation of Ebola virus reveals a capacity for extensive, modular polyploidy. PLoS ONE. 2012; 7(1):e29608. https://doi.org/10.1371/journal.pone.0029608 PMID: 22247782

32. Radwanska MJ, Jaskolowski M, Davydova E, Derewenda U, Miyake T, Engel DA, et al. The structure of the C-terminal domain of the nucleoprotein from the Bundibugyo strain of the Ebola virus in complex

with a pan-specific synthetic Fab. Acta Crystallogr D Struct Biol. 2018; 74(Pt 7):681–689. https://doi.org/10.1107/S2059798318007878 PMID: 29968677

33. Xu C, Katyal N, Nesterova T, Perilla JR. Molecular determinants of Ebola nucleocapsid stability from molecular dynamics simulations. J Chem Phys. 2020; 153(15):155102. https://doi.org/10.1063/5.0021491 PMID: 33092380

34. Licata JM, Johnson RF, Han Z, Harty RN. Contribution of ebola virus glycoprotein, nucleoprotein, and VP24 to budding of VP40 virus-like particles. J Virol. 2004; 78(14):7344–7351. https://doi.org/10.1128/JVI.78.14.7344-7351.2004 PMID: 15220407

35. Miyake T, Farley CM, Neubauer BE, Beddow TP, Hoenen T, Engel DA, et al. Ebola Virus Inclusion Body Formation and RNA Synthesis Are Controlled by a Novel Domain of Nucleoprotein Interacting with VP35. J Virol. 2020;94(16). https://doi.org/10.1128/JVI.02100-19 PMID: 32493824

36. Noda T, Watanabe S, Sagara H, Kawaoka Y. Mapping of the VP40-binding regions of the nucleoprotein of Ebola virus. J Virol. 2007; 81(7):3554–3562. https://doi.org/10.1128/JVI.02183-06 PMID: 17229682

37. Shi W, Huang Y, Sutton-Smith M, Tissot B, Panico M, Morris HR, et al. A filovirus-unique region of Ebola virus nucleoprotein confers aberrant migration and mediates its incorporation into virions. J Virol. 2008; 82(13):6190–6199. https://doi.org/10.1128/JVI.02731-07 PMID: 18417588

38. Wu L, Jin D, Wang D, Jing X, Gong P, Qin Y, et al. The two-stage interaction of Ebola virus VP40 with nucleoprotein results in a switch from viral RNA synthesis to virion assembly/budding. Protein Cell. 2020.

39. Kruse T, Biedenkopf N, Hertz EPT, Dietzel E, Stalmann G, López-Méndez B, et al. The Ebola Virus Nucleoprotein Recruits the Host PP2A-B56 Phosphatase to Activate Transcriptional Support Activity of VP30. Mol Cell. 2018; 69(1):136–145 e6. https://doi.org/10.1016/j.molcel.2017.11.034 PMID: 29290611

40. Welsch S, Kolesnikova L, Krahling V, Riches JD, Becker S, Briggs JAG, et al. Electron tomography reveals the steps in filovirus budding. PLoS Pathog. 2010; 6(4):e1000875. https://doi.org/10.1371/journal.ppat.1000875 PMID: 20442788

41. Dolnik O, Kolesnikova L, Becker S. Filoviruses: Interactions with the host cell. Cell Mol Life Sci. 2008; 65(5):756–776. https://doi.org/10.1007/s00018-007-7406-2 PMID: 18158582

42. Noda T, Kolesnikova L, Becker S, Kawaoka Y. The importance of the NP: VP35 ratio in Ebola virus nucleocapsid formation. J Infect Dis. 2011; 204(Suppl 3):S878–S883. https://doi.org/10.1093/infdis/jir310 PMID: 21987764

43. Alberti S. Phase separation in biology. Curr Biol. 2017; 27(20):R1097–R1102. https://doi.org/10.1016/j.cub.2017.08.069 PMID: 29065286

44. Alberti S, Gladfelter A, Mittag T. Considerations and Challenges in Studying Liquid-Liquid Phase Separation and Biomolecular Condensates. Cell. 2019; 176(3):419–434. https://doi.org/10.1016/j.cell.2018.12.035 PMID: 30682370

45. Feng Z, Chen X, Wu X, Zhang M. Formation of biological condensates via phase separation: Characteristics, analytical methods, and physiological implications. J Biol Chem. 2019; 294(40):14823–14835. https://doi.org/10.1074/jbc.REV119.007895 PMID: 31444270

46. Dolnik O, Gerresheim GK, Biedenkopf N. New Perspectives on the Biogenesis of Viral Inclusion Bodies in Negative-Sense RNA Virus Infections. Cell. 2021; 10(6). https://doi.org/10.3390/cells10061460 PMID: 34200781

47. Becker S, Rinne C, Hofsass U, Klenk HD, Muhlberger E. Interactions of Marburg virus nucleocapsid proteins. Virology. 1998; 249(2):406–417. https://doi.org/10.1006/viro.1998.9328 PMID: 9791031

48. Groseth A, Charton JE, Sauerborn M, Feldmann F, Jones SM, Hoenen T, et al. The Ebola virus ribonucleoprotein complex: a novel VP30-L interaction identified. Virus Res. 2009; 140(1–2):8–14. https://doi.org/10.1016/j.virusres.2008.10.017 PMID: 19041915

49. Etibor TA, Yamauchi Y, Amorim MJ. Liquid Biomolecular Condensates and Viral Lifecycles: Review and Perspectives. Viruses. 2021; 13(3). https://doi.org/10.3390/v13030366 PMID: 33669141

50. Kirchdoerfer RN, Abelson DM, Li S, Wood MR, Saphire EO. Assembly of the Ebola Virus Nucleoprotein from a Chaperoned VP35 Complex. Cell Rep. 2015; 12(1):140–149. https://doi.org/10.1016/j.celrep.2015.06.003 PMID: 26119732

51. Leung DW, Borek D, Luthra P, Binning JM, Anantpadma M, Liu G, et al. An Intrinsically Disordered Peptide from Ebola Virus VP35 Controls Viral RNA Synthesis by Modulating Nucleoprotein-RNA Interactions. Cell Rep. 2015; 11(3):376–389. https://doi.org/10.1016/j.celrep.2015.03.034 PMID: 25865894

52. Liu B, Dong S, Li G, Wang W, Liu X, Wang Y, et al. Structural Insight into Nucleoprotein Conformation Change Chaperoned by VP35 Peptide in Marburg Virus. J Virol. 2017; 91(16). https://doi.org/10.1128/JVI.00825-17 PMID: 28566377

53. Prins KC, Binning JM, Shabman RS, Leung DW, Amarasinghe GK, Basler CF, et al. Basic residues within the ebolavirus VP35 protein are required for its viral polymerase cofactor function. J Virol. 2010; 84(20):10581–10591. https://doi.org/10.1128/JVI.00925-10 PMID: 20686031

54. Leung DW, Ginder ND, Fulton DB, Nix J, Basler CF, Honzatko RB, et al. Structure of the Ebola VP35 interferon inhibitory domain. Proc Natl Acad Sci U S A. 2009; 106(2):411–416. https://doi.org/10.1073/pnas.0807854106 PMID: 19122151

55. Trunschke M, Conrad D, Enterlein S, Olejnik J, Brauburger K, Mühlberger E, et al. The L-VP35 and L-L interaction domains reside in the amino terminus of the Ebola virus L protein and are potential targets for antivirals. Virology. 2013; 441(2):135–145. https://doi.org/10.1016/j.virol.2013.03.013 PMID: 23582637

56. Heinrich BS, Cureton DK, Rahmeh AA, Whelan SP. Protein expression redirects vesicular stomatitis virus RNA synthesis to cytoplasmic inclusions. PLoS Pathog. 2010; 6(6):e1000958. https://doi.org/10.1371/journal.ppat.1000958 PMID: 20585632

57. Guryanov SG, Liljeroos L, Kasaragod P, Kajander T, Butcher SJ. Crystal Structure of the Measles Virus Nucleoprotein Core in Complex with an N-Terminal Region of Phosphoprotein. J Virol. 2015; 90 (6):2849–2857. https://doi.org/10.1128/JVI.02865-15 PMID: 26719278

58. Xu W, Luthra P, Wu C, Batra J, Leung DW, Basler CF, et al. Ebola virus VP30 and nucleoprotein interactions modulate viral RNA synthesis. Nat Commun. 2017; 8:15576. https://doi.org/10.1038/ncomms15576 PMID: 28593988

59. Lier C, Becker S, Biedenkopf N. Dynamic phosphorylation of Ebola virus VP30 in NP-induced inclusion bodies. Virology. 2017; 512:39–47. https://doi.org/10.1016/j.virol.2017.09.006 PMID: 28915404

60. Hartlieb B, Muziol T, Weissenhorn W, Becker S. Crystal structure of the C-terminal domain of Ebola virus VP30 reveals a role in transcription and nucleocapsid association. Proc Natl Acad Sci U S A. 2007; 104(2):624–629. https://doi.org/10.1073/pnas.0606730104 PMID: 17202263

61. Modrof J, Mühlberger E, Klenk H-D, Becker S. Phosphorylation of VP30 impairs ebola virus transcription. J Biol Chem. 2002; 277(36):33099–33104. https://doi.org/10.1074/jbc.M203775200 PMID: 12052831

62. Mühlberger E, Lötfering B, Klenk HD, Becker S. Three of the four nucleocapsid proteins of Marburg virus, NP, VP35, and L, are sufficient to mediate replication and transcription of Marburg virus-specific monocistronic minigenomes. J Virol. 1998; 72(11):8756–8764. https://doi.org/10.1128/JVI.72.11.8756-8764.1998 PMID: 9765419

63. Biedenkopf N, Hartlieb B, Hoenen T, Becker S. Phosphorylation of Ebola virus VP30 influences the composition of the viral nucleocapsid complex: impact on viral transcription and replication. J Biol Chem. 2013; 288(16):11165–11174. https://doi.org/10.1074/jbc.M113.461285 PMID: 23493393

64. Biedenkopf N, Lier C, Becker S. Dynamic Phosphorylation of VP30 Is Essential for Ebola Virus Life Cycle. J Virol. 2016; 90(10):4914–4925. https://doi.org/10.1128/JVI.03257-15 PMID: 26937028

65. Takamatsu Y, Krähling V, Kolesnikova L, Halwe S, Lier C, Baumeister S, et al. Serine-Arginine Protein Kinase 1 Regulates Ebola Virus Transcription. MBio. 2020; 11(1). https://doi.org/10.1128/mBio.02565-19 PMID: 32098814

66. Nelson EV, Schmidt KM, Deflube LR, Doganay S, Banadyga L, Olejnik J, et al. Ebola Virus Does Not Induce Stress Granule Formation during Infection and Sequesters Stress Granule Proteins within Viral Inclusions. J Virol. 2016; 90(16):7268–7284. https://doi.org/10.1128/JVI.00459-16 PMID: 27252530

67. Fricke J, Koo LY, Brown CR, Collins PL. p38 and OGT sequestration into viral inclusion bodies in cells infected with human respiratory syncytial virus suppresses MK2 activities and stress granule assembly. J Virol. 2013; 87(3):1333–1347. https://doi.org/10.1128/JVI.02263-12 PMID: 23152511

68. Lifland AW, Jung J, Alonas E, Zurla C, Crowe J.E. Jr., Santangelo PJ, et al. (2012) Human respiratory syncytial virus nucleoprotein and inclusion bodies antagonize the innate immune response mediated by MDA5 and MAVS. J Virol 86 (15):8245–8258. https://doi.org/10.1128/JVI.00215-12 PMID: 22623778

69. Lindquist ME, Lifland AW, Utley TJ, Santangelo PJ, Crowe J.E. Jr. (2010) Respiratory syncytial virus induces host RNA stress granules to facilitate viral replication. J Virol 84 (23): 12274–12284. https://doi.org/10.1128/JVI.00260-10 PMID: 20844027

70. Rincheval V, Lelek M, Gault E, Bouillier C, Sitterlin D, Blouquit-Laye S, et al. Functional organization of cytoplasmic inclusion bodies in cells infected by respiratory syncytial virus. Nat Commun. 2017; 8 (1):563. https://doi.org/10.1038/s41467-017-00655-9 PMID: 28916773

71. Banadyga L, Hoenen T, Ambroggio X, Dunham E, Groseth A, Ebihara H, et al. Ebola virus VP24 interacts with NP to facilitate nucleocapsid assembly and genome packaging. Sci Rep. 2017; 7(1):7698. https://doi.org/10.1038/s41598-017-08167-8 PMID: 28794491

72. Bamberg S, Kolesnikova L, Moller P, Klenk HD, Becker S. VP24 of Marburg virus influences formation of infectious particles. J Virol. 2005; 79(21):13421–13433. https://doi.org/10.1128/JVI.79.21.13421-13433.2005 PMID: 16227263

73. Hoenen T, Jung S, Herwig A, Groseth A, Becker S. Both matrix proteins of Ebola virus contribute to the regulation of viral genome replication and transcription. Virology. 2010; 403(1):56–66. https://doi.org/10.1016/j.virol.2010.04.002 PMID: 20444481

74. Mateo M, Carbonnelle C, Martinez MJ, Reynard O, Page A, Volchkova VA, et al. Knockdown of Ebola virus VP24 impairs viral nucleocapsid assembly and prevents virus replication. J Infect Dis. 2011; 204 (Suppl 3):S892–S896. https://doi.org/10.1093/infdis/jir311 PMID: 21987766

75. Watt A, Moukambi F, Banadyga L, Groseth A, Callison J, Herwig A, et al. A novel life cycle modeling system for Ebola virus shows a genome length-dependent role of VP24 in virus infectivity. J Virol. 2014; 88(18):10511–10524. https://doi.org/10.1128/JVI.01272-14 PMID: 24965473

76. Watanabe S, Noda T, Halfmann P, Jasenosky L, Kawaoka Y. Ebola virus (EBOV) VP24 inhibits transcription and replication of the EBOV genome. J Infect Dis. 2007; 196(Suppl 2):S284–S290. https://doi.org/10.1086/520582 PMID: 17940962

77. Vidal S, El Motiam A, Seoane R, Preitakaite V, Bouzaher YH, Gómez-Medina S, et al. Regulation of the Ebola Virus VP24 Protein by SUMO. J Virol. 2019; 94(1). https://doi.org/10.1128/JVI.01687-19 PMID: 31597768

78. Harrison AR, David CT, Rawlinson SM, Moseley GW. The Ebola Virus Interferon Antagonist VP24 Undergoes Active Nucleocytoplasmic Trafficking. Viruses. 2021; 13(8). https://doi.org/10.3390/v13081650 PMID: 34452514

79. Takamatsu Y, Kolesnikova L, Becker S. Ebola virus proteins NP, VP35, and VP24 are essential and sufficient to mediate nucleocapsid transport. Proc Natl Acad Sci U S A. 2018; 115(5):1075–1080. https://doi.org/10.1073/pnas.1712263115 PMID: 29339477

80. Takamatsu Y, Dolnik O, Noda T, Becker S. A live-cell imaging system for visualizing the transport of Marburg virus nucleocapsid-like structures. Virol J. 2019; 16(1):159. https://doi.org/10.1186/s12985-019-1267-9 PMID: 31856881

81. Welch MD, Way M. Arp2/3-mediated actin-based motility: a tail of pathogen abuse. Cell Host Microbe. 2013; 14(3):242–255. https://doi.org/10.1016/j.chom.2013.08.011 PMID: 24034611

82. Suetsugu S. Activation of nucleation promoting factors for directional actin filament elongation: allosteric regulation and multimerization on the membrane. Semin Cell Dev Biol. 2013; 24(4):267–271. https://doi.org/10.1016/j.semcdb.2013.01.006 PMID: 23380397

83. Grikscheit K, Dolnik O, Takamatsu Y, Pereira AR, Becker S. Ebola Virus Nucleocapsid-Like Structures Utilize Arp2/3 Signaling for Intracellular Long-Distance Transport. Cell. 2020; 9(7). https://doi.org/10.3390/cells9071728 PMID: 32707734

84. Mueller J, Pfanzelter J, Winkler C, Narita A, Le Clainche C, Nemethova M, et al. Electron tomography and simulation of baculovirus actin comet tails support a tethered filament model of pathogen propulsion. PLoS Biol. 2014; 12(1):e1001765. https://doi.org/10.1371/journal.pbio.1001765 PMID: 24453943

85. Dolnik O, Kolesnikova L, Welsch S, Strecker T, Schudt G, Becker S, et al. Interaction with Tsg101 is necessary for the efficient transport and release of nucleocapsids in marburg virus-infected cells. PLoS Pathog. 2014; 10(10):e1004463. https://doi.org/10.1371/journal.ppat.1004463 PMID: 25330247

86. Kolesnikova L, Bohil AB, Cheney RE, Becker S. Budding of Marburgvirus is associated with filopodia. Cell Microbiol. 2007; 9(4):939–951. https://doi.org/10.1111/j.1462-5822.2006.00842.x PMID: 17140405

87. Mattila PK, Lappalainen P. Filopodia: molecular architecture and cellular functions. Nat Rev Mol Cell Biol. 2008; 9(6):446–454. https://doi.org/10.1038/nrm2406 PMID: 18464790

88. Berg JS, Cheney RE. Myosin-X is an unconventional myosin that undergoes intrafilopodial motility. Nat Cell Biol. 2002; 4(3):246–250. https://doi.org/10.1038/ncb762 PMID: 11854753

89. Takamatsu Y, Kolesnikova L, Schauflinger M, Noda T, Becker S. The Integrity of the YxxL Motif of Ebola Virus VP24 Is Important for the Transport of Nucleocapsid-Like Structures and for the Regulation of Viral RNA Synthesis. J Virol. 2020; 94(9). https://doi.org/10.1128/JVI.02170-19 PMID: 32102881

90. Dietzel E, Kolesnikova L, Maisner A. Actin filaments disruption and stabilization affect measles virus maturation by different mechanisms. Virol J. 2013; 10:249. https://doi.org/10.1186/1743-422X-10-249 PMID: 23914985

91. Yacovone SK, Smelser AM, Macosko JC, Holzwarth G, Ornelles DA, Lyles DS, et al. Migration of Nucleocapsids in Vesicular Stomatitis Virus-Infected Cells Is Dependent on both Microtubules and Actin Filaments. J Virol. 2016; 90(13):6159–6170. https://doi.org/10.1128/JVI.00488-16 PMID: 27122580

92. Ohkawa T, Volkman LE, Welch MD. Actin-based motility drives baculovirus transit to the nucleus and cell surface. J Cell Biol. 2010; 190(2):187–195. https://doi.org/10.1083/jcb.201001162 PMID: 20660627

93. Marek M, Merten OW, Galibert L, Vlak JM, van Oers MM. Baculovirus VP80 protein and the F-actin cytoskeleton interact and connect the viral replication factory with the nuclear periphery. J Virol. 2011; 85(11):5350–5362. https://doi.org/10.1128/JVI.00035-11 PMID: 21450830

94. Goley ED, Ohkawa T, Mancuso J, Woodruff JB, D'Alessio JA, Cande WZ, et al. Dynamic nuclear actin assembly by Arp2/3 complex and a baculovirus WASP-like protein. Science. 2006; 314(5798):464–467. https://doi.org/10.1126/science.1133348 PMID: 17053146

95. Whelan SP, Wertz GW. Transcription and replication initiate at separate sites on the vesicular stomatitis virus genome. Proc Natl Acad Sci U S A. 2002; 99(14):9178–9183. https://doi.org/10.1073/pnas.152155599 PMID: 12089339

96. Tremaglio CZ, Noton SL, Deflube LR, Fearns R. Respiratory syncytial virus polymerase can initiate transcription from position 3 of the leader promoter. J Virol. 2013; 87(6):3196–3207. https://doi.org/10.1128/JVI.02862-12 PMID: 23283954

97. Hodges J, Tang X, Landesman MB, Ruedas JB, Ghimire A, Gudheti MV, et al. Asymmetric packaging of polymerases within vesicular stomatitis virus. Biochem Biophys Res Commun. 2013; 440(2):271–276. https://doi.org/10.1016/j.bbrc.2013.09.064 PMID: 24055706

98. Kolesnikova L, Mittler E, Schudt G, Shams-Eldin H, Becker S. Phosphorylation of Marburg virus matrix protein VP40 triggers assembly of nucleocapsids with the viral envelope at the plasma membrane. Cell Microbiol. 2012; 14(2):182–197. https://doi.org/10.1111/j.1462-5822.2011.01709.x PMID: 21981045

99. Dolnik O, Kolesnikova L, Stevermann L, Becker S. Tsg101 is recruited by a late domain of the nucleocapsid protein to support budding of Marburg virus-like particles. J Virol. 2010; 84(15):7847–7856. https://doi.org/10.1128/JVI.00476-10 PMID: 20504928